

Solubilities and thermophysical properties of ionic liquids*

Urszula Domańska[‡]

Physical Chemistry Division, Faculty of Chemistry, Warsaw University of Technology, Noakowskiego 3, 00-664 Warsaw, Poland

Abstract: This report presents the systematic study on the solubilities of 1-alkyl-3-methylimidazolium hexafluorophosphate [e, or bmim][PF₆], 1-alkyl-3-methylimidazolium methylsulfate [almim][CH₃SO₄], 1-hexyloxymethyl-3-methylimidazolium ionic liquids (ILs) [C₆H₁₃OCH₂mim][BF₄], or [C₆H₁₃OCH₂mim][(CF₃SO₂)₂N] in aliphatic hydrocarbons (heptane, octane), cyclohydrocarbons (cyclopentane, cyclohexane) and aromatic hydrocarbons (benzene, toluene, ethylbenzene, *o*-xylene, *m*-xylene, *p*-xylene), and in alcohols (methanol, ethanol, propan-1-ol, propan-2-ol, butan-1-ol, butan-2-ol, *tert*-butyl alcohol, and 3-methylbutan-1-ol) as well as of 1-alkyl-3-methylimidazolium chloride [C₄, C₁₀, or C₁₂mim][Cl] in alcohols. The solubilities have been measured by a dynamic method from 290 K to the melting point of IL or to the boiling point of the solvent. The solubility of [emim][PF₆] and [bmim][PF₆] in aromatic hydrocarbons decreases with an increase of the molecular weight of the solvent. The difference on the solubility in *o*-, *m*-, and *p*-xylene is not significant. The solubility of [emim][PF₆] in alcohols decreases with an increase of the molecular weight of the solvent and is higher in secondary alcohols than in primary alcohols. In every case, with the exception of methanol, the mutual liquid–liquid equilibrium was observed. The shape of the equilibrium curve is similar for [emim][PF₆] in every alcohol. The observations of upper critical solution temperatures were limited by the boiling temperature of the solvent. For example, for [emim][PF₆], solubilities in methanol and ethanol are higher than that in aromatic hydrocarbons. The miscibility gap for C₃ alcohols is higher than that in benzene, but comparable with the solubility in toluene; solubility in 3-methylbutan-1-ol is very similar to ethylbenzene and *o*-, *m*-, and *p*-xylene.

The data were correlated by means of the UNIQUAC and modified nonrandom two-liquid (NRTL) equations utilizing parameters derived from the solid–liquid equilibrium (SLE). The root-mean-square deviations of the solubility temperatures for all calculated data depend on the particular system and the equation used.

The solubilities of [C₄, C₁₀, or C₁₂mim][Cl] and alkyl-(2-hydroxyethyl)-dimethylammonium ILs in octan-1-ol and water have been measured and used to calculate the octan-1-ol/water partition coefficients as a function of temperature and alkyl substituent. Experimental partition coefficients (log *P*) are negative for imidazoles, 1,3-dialkylimidazolium chlorides, and investigated ammonium salts. Good knowledge of ILs permits the elimination of volatile organic compounds and makes chemistry cleaner and greener.

Keywords: green chemistry; ionic liquids; liquid–liquid equilibria; solid–liquid equilibria; phase diagrams.

*Paper based on a presentation at the 11th International Symposium on Solubility Phenomena (11th ISSP), Aveiro, Portugal, 25–29 July 2004. Other presentations are published in this issue, pp. 513–665.

[‡]E-mail: ula@ch.pw.edu.pl

INTRODUCTION

Ionic liquids (ILs) are a new generation of solvents for catalysis and synthesis that have been demonstrated as potential successful replacements for conventional media in chemical processes [1–13]. They are generally salts based on a substituted imidazolium, or pyridinium cation and an inorganic anion such as halide, $[\text{AlCl}_4]^-$, $[\text{BF}_4]^-$, or $[\text{PF}_6]^-$ and are very often liquids at room temperature. Room-temperature ILs are being investigated as more clean replacements for volatile organic solvents (VOCs). The important properties include high heat capacity, high density, extremely low volatility, nonflammability, high thermal stability, wide temperature range for liquid, many variations in compositions, and a large number of possible variations in cation and anion conformation, allowing fine-tuning of the IL properties for specific applications [14–28]. A major reason for the interest in ILs is their negligible vapor pressure, which decreases the risk of technological exposure and the loss of solvent to the atmosphere. With their promising physical and chemical properties, ILs are versatile electrolytes for diverse technologies, e.g., in batteries, photoelectrical cells, and other electrochemical devices [29–34]. Of course, the presence of water in the gas phase or in the IL has a considerable impact on the electrochemical and physicochemical properties of IL. Properties for an “ideal” IL were thought to include low cost, water stability (as well as stability to solvents, products, etc.), low toxicity, low environmental impact, noncorrosive, and recyclable. Industry representatives suggested a viscosity of less than 100 centipoises and thermal stability to 973 K (although a lower limit of ca. 473 K would be fine for general use) as additional ideal requirements. Physical and thermodynamic properties and constants, transport properties, miscibilities, and purity assessment were highlighted as immediate needs. The solid–liquid and liquid–liquid measurements of IL systems based on *N,N*-dialkyl-substituted imidazolium cations or ammonium cations are attracting increasing attention for applications in liquid–liquid extraction [35–43]. There are first publications about the suitability of ILs as entrainers for the extractive distillation and as extraction solvents for the liquid–liquid extraction. ILs were found to be capable of breaking a multitude of azeotropic systems. The nonvolatility of ILs in combination with their remarkable separation efficiency and selectivity enable new processes for the separation of azeotropic mixtures which, in comparison to conventional separation processes, might offer a potential for cost savings. Until now, it cannot be predicted which IL is the best one for certain applications. With increasing comprehension on how the structure of an IL affects its physical properties, one will be able to use the advantages of ILs in comparison to VOCs. Owing to their unique structures and properties, they may be compared with dendrimers or hyperbranched polymers. For example, it is possible to extract out of a THF–water mixture using $[\text{emim}][\text{BF}_4]$. This IL easily breaks the azeotropic ethanol–water phase behavior by interacting selectively with water. (The conventional entrainer is 1,2-ethanediol). The different interactions IL–water and IL–THF result not only in an increasing relative volatility of THF, but also in a phase split of the liquid mixture [44]. It was shown also that ILs may give much higher selectivities for the separation of aliphatics from aromatics (cyclohexane/benzene) than NMP or (NMP + water) mixture [45]. The large miscibility gap exists in the mixtures of 1-ethyl-3-methylimidazolium bis(trifluoromethylsulfonyl)imide, $[\text{emim}][(\text{CF}_3\text{SO}_2)_2\text{N}]$, or 1-ethyl-3-methylimidazolium ethyl-sulfate, $[\text{emim}][\text{C}_2\text{H}_5\text{SO}_4]$ with aliphatic (cyclohexane) and aromatic (benzene) hydrocarbons [45]. The excess molar enthalpy for the benzene + $[\text{emim}][(\text{CF}_3\text{SO}_2)_2\text{N}]$ was highly negative (about $-750 \text{ J}\cdot\text{mol}^{-1}$) and for the cyclohexane + $[\text{emim}][(\text{CF}_3\text{SO}_2)_2\text{N}]$ was positive (about $450 \text{ J}\cdot\text{mol}^{-1}$) [45]. This means that ILs are excellent entrainers for the separation of aliphatic from aromatic hydrocarbons by extractive distillation or extraction.

ILs were also used as an alternative solvent to study liquid–liquid extraction of heavy metal ions. Dithizone was employed as a metal chelator to form neutral metal-dithizone complexes with heavy metal ions to extract metal ions from aqueous solutions to IL ($[\text{bmim}][\text{PF}_6]$). This extraction is possible due to the high distribution ratios of the metal complexes between $[\text{bmim}][\text{PF}_6]$ and aqueous phase [46]. This was a pH-dependent process.

This paper follows the discussion on room-temperature ILs, and is a continuation of our systematic study of the ILs solubility measurements [47–51]. In our previous work, the solubility of 1-ethyl-3-methylimidazolium hexafluorophosphate, [emim][PF₆], in aromatic hydrocarbons (benzene, toluene, ethylbenzene, and *o*-, *m*-, and *p*-xylene) and of 1-butyl-3-methylimidazolium hexafluorophosphate, [bmim][PF₆], in the same aromatic hydrocarbons, and in *n*-alkanes (pentane, hexane, heptane, octane) and in cyclohydrocarbons (cyclopentane, cyclohexane) has been measured [39]. Also, the solubilities of [emim][PF₆] in alcohols (methanol, ethanol, propan-1-ol, propan-2-ol, butan-1-ol, butan-2-ol, *tert*-butyl alcohol, and 3-methylbutan-1-ol) was measured [40]. Our liquid–liquid equilibrium (LLE) measurements of [emim][PF₆] or [bmim][PF₆] have shown mutual solubilities with aliphatic, cyclic, and aromatic hydrocarbons, being a function of the chain length of the alkyl substituent at the imidazole ring [39,40]. The solubility of [emim][PF₆] in alcohols decreases with an increase of the molecular weight of the solvent and is higher in secondary alcohols than in primary alcohols. In every case, with the exception of methanol, the mutual LLE was observed. The shape of the equilibrium curve was similar for [emim][PF₆] in every alcohol. The observation of upper critical solution temperature (UCST) was limited by the boiling temperature of the solvent. The solubility of [emim][PF₆] and [bmim][PF₆] in aromatic hydrocarbons and in alcohols decreases with an increase of the molecular weight of the solvent. The difference in the solubility in *o*-, *m*- and *p*-xylene was not significant. The solubility of [emim][PF₆] in alcohols, with the exception of methanol, show the mutual LLE. Solubility is better in secondary alcohols than in primary alcohols. For example, for [emim][PF₆], solubilities in methanol and ethanol are higher than that in aromatic hydrocarbons. The miscibility gap in C₃ alcohols is bigger than that in benzene, but comparable with the solubility in toluene; solubility in 3-methyl-butanol-1 is very low and similar to ethylbenzene and *o*-, *m*-, and *p*-xylene [39,40].

At the same time, the solid–liquid equilibria of 1-butyl-, decyl-, or dodecyl-3-methylimidazolium chloride [C₄, C₁₀, C₁₂ mim][Cl] in alcohols has been measured by the dynamic method [47–50]. The experimental solid–liquid equilibrium (SLE) phase diagrams investigated for [C₄ or C₁₀ or C₁₂ mim][Cl] have shown that the solubility of IL in alcohols decreases with an increase of the carbon chain of an alcohol from C₂ to C₈, with the exception of the solubility of [bmim][Cl] in butan-1-ol. The [bmim][Cl] exhibits the best solubility in butan-1-ol, which can be explained by the best packing effect in the solution for the same number of carbon atoms in the solvent and butyl substituent at the imidazolium ring. Solubility of [bmim][Cl] in longer-chain alcohols is similar to that in octan-1-ol. The liquidus curves of the primary, secondary, and tertiary alcohols exhibit similar shapes. The solubility increases in the order butan-1-ol > butan-2-ol > *tert*-butyl alcohol [50]. Positive and negative deviations from the ideality were found, thus, the solubility was higher or partly higher than the ideal one in ethanol, butan-1-ol, butan-2-ol, and *tert*-butyl alcohol and was lower than the ideal solubility in other alcohols. The complete phase diagrams [C₄, C₁₀, or C₁₂ mim][Cl] were found to show eutectic behavior for {[C₄, C₁₀, or C₁₂ mim][Cl] + *tert*-butyl alcohol, or decan-1-ol, or dodecan-1-ol} [47,48–50]. The solubilities of [C₁₂mim][Cl] in hydrocarbons (benzene, octane, decane, dodecane), ethers {dipropyl ether, methyl 1,1-dimethylethyl ether (MTBE), methyl 1,1-dimethylpropyl ether (MTAE), tetrahydrofuran, (THF)} have been also measured [51]. The huge influence of the anion {[Cl][−], [PF₆][−], [CH₃SO₄][−]} on the solubility of 1-butyl-3-methylimidazolium salts in dipropyl ether was observed [51].

The results of solid–liquid equilibria in all of our papers [39,40,47–51] were correlated by means of the different G^E models, mainly by the Wilson equation [52], two modified nonrandom two-liquid (NRTL) equations [53], and the UNIQUAC ASM equation [54].

The melting point, the glass transition temperature, enthalpy of fusion, and enthalpies of different solid–solid phase transitions were determined by the differential scanning calorimetry (DSC) for every IL under study.

For a better understanding of the IL behavior and with a view to the application in chemical engineering or the development of thermodynamic models, reliable experimental data are required. Basic

ILs can act as both a hydrogen bond acceptor (anion) and donor (cation) and would be expected to interact with solvents with both accepting and donating sites. On the other hand, polar solvents as alcohols are very well known to form hydrogen-bonded net with both high enthalpies and constants of association. Hence, they would be expected to stabilize with hydrogen bond donor sites. That was the new idea of this work—increasing hydrogen-bonding opportunities with the anion by replacement of $[\text{Cl}]^-$ and $[\text{PF}_6]^-$ anions by $[\text{CH}_3\text{SO}_4]^-$ with four atoms of oxygen, or with the cation by adding the alkoxy group to the alkane chain at the imidazole ring, $[\text{C}_6\text{H}_{13}\text{OCH}_2\text{mim}]^+$.

This work is a continuation of our previous study [47–51], which focused on understanding which features control the liquid–liquid phase equilibrium of imidazolium-based ILs with different organic solvents. The characteristics investigated here include the effect of alkyl chain length of the cation (methyl vs. butyl), the effect of the oxygen substitution on one chain of the cation ($[\text{C}_6\text{H}_{13}\text{OCH}_2\text{mim}]^+$), and the effect of anion ($[\text{BF}_4]^-$ vs. $[(\text{CF}_3\text{SO}_2)_2\text{N}]^-$) or ($[\text{PF}_6]^-$ vs. $[\text{CH}_3\text{SO}_4]^-$).

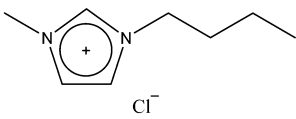
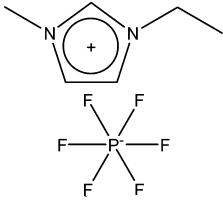
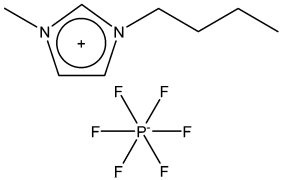
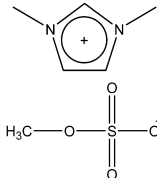
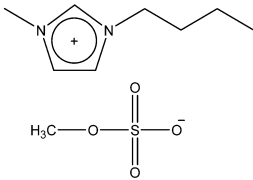
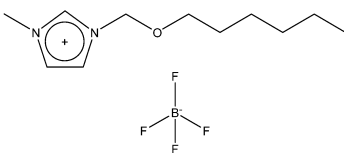
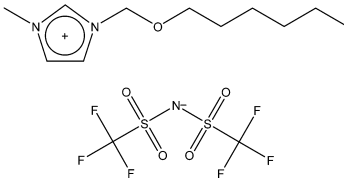
EXPERIMENTAL PROCEDURES AND RESULTS

Materials

The 1,3-dialkylimidazolium hexafluorophosphate $[\text{almim}][\text{PF}_6]$, chloride $[\text{almim}][\text{Cl}]$, or methylsulfate $[\text{almim}][\text{CH}_3\text{SO}_4]$ samples were obtained from Solvent Innovation GmbH, Köln, Germany. The sample's purity was ≥ 98 mass %, and they were used without any purification. The substances were packed under the nitrogen. The other ILs were synthesized. 1-Hexyloxymethyl-3-methylimidazolium tetrafluoroborate, $[\text{C}_6\text{H}_{13}\text{OCH}_2\text{mim}][\text{BF}_4]$, or bis(trifluoromethylsulfonyl)imide $[\text{C}_6\text{H}_{13}\text{OCH}_2\text{mim}][(\text{CF}_3\text{SO}_2)_2\text{N}]$ $\{[(\text{CF}_3\text{SO}_2)_2\text{N}] = [\text{Tf}_2\text{N}]\}$ were obtained from 1-hexyloxymethyl-3-methylimidazolium chloride [55,56]. The prepared ILs were characterized by their ^1H NMR and ^{13}C NMR spectra. ^1H NMR spectra were recorded on a Varian Model XL 300 spectrometer at 300 MHz with tetramethylsilane as the standard. ^{13}C NMR spectra were recorded on the same instrument at 75 MHz to confirm any major impurities. All ILs were cleaned with activated carbon to remove any colored compounds and dried under vacuum at 348.15 K for 48 h to remove organic solvents and water. Analysis for the water contamination using the Karl–Fischer technique for solvents and ILs showed that the impurity in each of the substances was < 0.02 mol %. Ionic liquids discussed in this work are presented in Table 1.

All solvents were delivered from Sigma Aldrich Chemie GmbH, Stenheim, Germany. Before direct use they were fractionally distilled over different drying reagents to the mass fraction purity ≥ 99.8 mass %. The solvents were stored over freshly activated molecular sieves of type 4 Å (Union Carbide).

Table 1 List of imidazolium-based ILs investigated.

1-butyl-3-methylimidazolium chloride		[bmim][Cl]
1-ethyl-3-methylimidazolium hexafluoroborate		[emim][PF ₆]
1-butyl-3-methylimidazolium hexafluoroborate		[bmim][PF ₆]
1,3-dimethylimidazolium methylsulfate		[mmim][CH ₃ SO ₄]
1-butyl-3-methylimidazolium methylsulfate		[bmim][CH ₃ SO ₄]
1-hexyloxymethyl-3-methylimidazolium tetrafluoroborate		[C ₆ H ₁₃ OCH ₂ mim][BF ₄]
1-hexyloxymethyl-3-methylimidazolium bis(trifluoromethylsulfonyl)imide,		[C ₆ H ₁₃ OCH ₂ mim] [(CF ₃ SO ₂) ₂ N]=[Tf ₂ N]

Solid–liquid and liquid–liquid equilibria apparatus measurements

SLE and LLE temperatures were determined using a dynamic method described in detail previously [47–51]. Appropriate mixtures of solute and solvent placed under the nitrogen in dry box into a Pyrex glass cell were heated very slowly (less than $2\text{ K}\cdot\text{h}^{-1}$ near the equilibrium temperature) with continuous stirring inside a cell which was placed in a glass thermostat filled with silicone, oil, or water. The temperature of the liquid bath was varied slowly until the last crystals disappeared. This temperature was taken as the temperature of the (solid–liquid) equilibrium in the saturated solution. The crystal disappearance temperatures were detected visually. In LLE measurements, a sample of known composition was placed in a view-cell and heated until it was one phase. The equilibrium temperature was two phases (foggy mixture) disappearance in the liquid phase, observed visually during increasing temperature. The observation of the “cloud point” with decreasing temperature was very difficult. The effect of precooling and kinetics of the phenomenon of binary-phase creation were the reasons that the temperature of “cloud point” was not repeatable during the experiment. The temperature was measured with an electronic thermometer P 550 (DOSTMANN Electronic GmbH) with the probe totally immersed in the thermostating liquid. The accuracy of the temperature measurements was judged to be $\pm 0.01\text{ K}$. Mixtures were prepared by mass, and the uncertainty in the composition was estimated to be ± 0.0005 and $\pm 0.5\text{ K}$ in the mole fraction and temperature, respectively. It was found that the solution-crystallization procedure was quite slow and difficult, thus the solubility measurements were very time-consuming. The LLE measurements were limited at the upper temperature by the boiling point of the solvent.

RESULTS AND DISCUSSION

For this discussion, the LLE for new binary IL–organic solvent systems were determined. The solubilities of [mmim][CH₃SO₄] or [bmim][CH₃SO₄] in alcohols, ethers, aromatic hydrocarbons, and heptane were measured and compared with previously measured [emim][PF₆] or [bmim][PF₆] data [39–41] or others salts, published by different authors. The results are shown in Figs. 1–9.

The ability of a polar anion to create the hydrogen bond with the alcohol significantly increases the solubilities of IL in solvent. The interaction of methylsulfate [CH₃SO₄][−] anion with alcohols is so strong that full miscibility was observed for [bmim][CH₃SO₄] in alcohols from methanol to undecan-1-ol and [mmim][CH₃SO₄] in alcohols from methanol to pentan-1-ol at room temperature. Only the binary systems of [mmim][CH₃SO₄] with alcohols from hexan-1-ol to undecan-1-ol exhibit UCST. One can assume that especially unsymmetrical cation [bmim]⁺ causes the enthalpic effects of miscibility (in which the strength of interactions play its main role) to be more responsible than entropic effects for higher A–B interaction than A–A and B–B interaction.

The influence of the cation's alkyl chain length was observed previously for [BF₄][−] and [Tf₂N][−] anions [57,58] and [PF₆][−] [39–41,59]. The decrease in the UCST of the system was observed with the increasing of the alkyl chain length on the cation. For [mmim][CH₃SO₄] or [bmim][CH₃SO₄] in alcohols from hexan-1-ol to undecan-1-ol, the same effect was observed. By lengthening the alkyl chain on the cation from methyl to butyl, complete miscibility was observed. Figure 1 presents the solubility of [mmim][CH₃SO₄] in hexan-1-ol and octan-1-ol. The UCST increases as the length of the alkyl chain of the alcohol increases and was shifted to the higher IL solute mole fraction. For mixtures of [bmim][PF₆], the miscibility gap was observed [41] with general trend of increasing UCST with an increasing alkyl chain length of an alcohol. This trend is consistent with other systems that have been investigated, including our previous study for [emim][PF₆] [40] and the study of [emim][Tf₂N] with primary alcohols [57]; for [bmim][BF₄] and [bmim][Tf₂N] with primary and secondary alcohols [58]; and the study of alkylimidazolium ILs with [BF₄][−] and [PF₆][−] anions [60]. These differences were shown for two examples in Fig. 1.

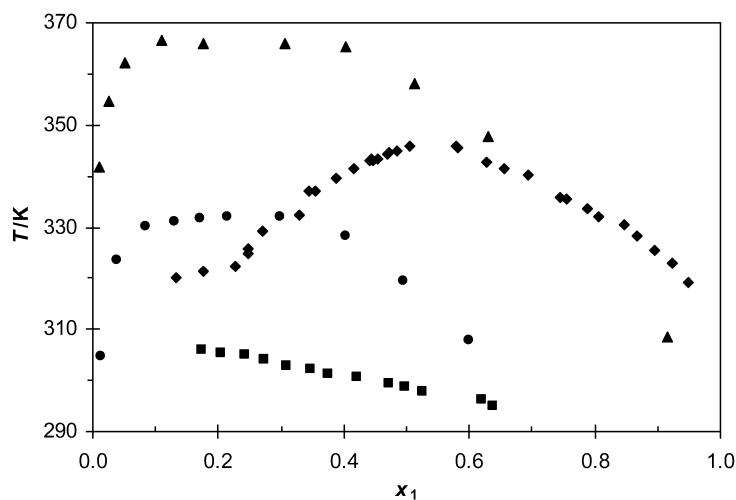


Fig. 1 T-x diagram for different ILs (1) in hexan-1-ol: ●, [bmim][Tf₂N] [58]; ▲, [bmim][BF₄] [58]; ■, [mmim][CH₃SO₄]; or in octan-1-ol ◆, [mmim][CH₃SO₄].

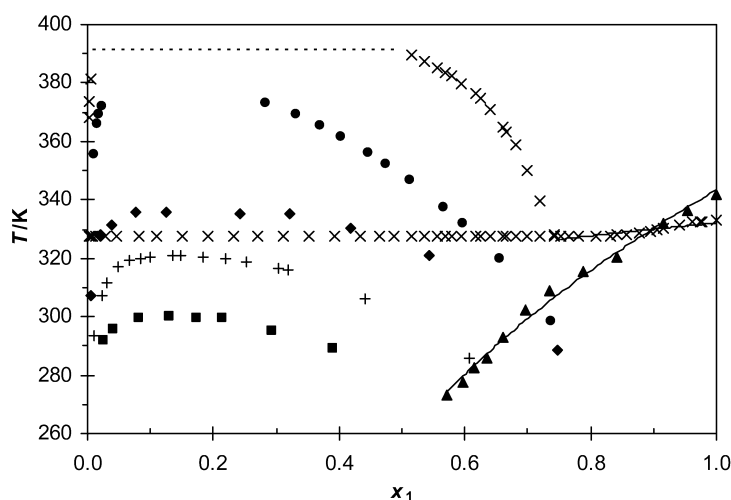


Fig. 2 Solid-liquid and liquid-liquid equilibrium diagrams for different ILs (1) in butan-1-ol: ■, [bmim][Tf₂N] [58]; ◆, [bmim][BF₄] [58]; ●, [bmim][PF₆] [41]; X, [emim][PF₆] [40]; +, [emim][Tf₂N] [57]; ▲, [bmim][Cl] [50]; solid line, calculated by the NRTL1 equation; dotted line, boiling temperature of butan-1-ol.

The comparison of the different IL solubilities is shown in Figs. 1 and 2. The LLE of [bmim][BF₄] and [bmim][Tf₂N] with hexan-1-ol [58] is shown in Fig. 1. For these two ILs, the UCST is 30 K ([bmim][Tf₂N]) or even 60 K higher ([bmim][BF₄]) than for [mmim][CH₃SO₄]. The stronger interaction with solvent was noted with [Tf₂N] anion [58]. There is no doubt, however, that four oxygen atoms in [CH₃SO₄]⁻ anion are responsible for stronger hydrogen bond formation with an alcohol.

Figure 2 presents some results of the solubility of different ILs in butan-1-ol. Solid [bmim][Cl] exhibits the best solubility in butan-1-ol between alcohols C₂-C₁₂ (packing effects) [50], whilst the other solid IL, [emim][PF₆], with very closed melting temperature exhibits the miscibility gap in butan-1-ol [40]. Melting temperatures are 341.94 K and 332.80 K for [bmim][Cl] and [emim][PF₆], respectively, thus, the liquidus curve of [emim][PF₆] shows slightly better solubility just below the melting

temperature, but for the other area, the liquidus curve is very flat and two liquid phases were observed for IL mole fraction from 0.002 to 0.74 (see Fig. 2). Only in methanol, the [emim][PF₆] was completely soluble [40]. The effect of the anion can be discussed by comparing the solubility data for a specific alcohol with different ILs having the same cation. Figure 2 presents the increasing solubility (decreasing UCST point) in the order: [emim][PF₆] < [emim][Tf₂N] and [bmim][PF₆] < [bmim][BF₄] < [bmim][Tf₂N].

This trend will keep order also for the weaker interactions of IL with the solvent. By changing the solvent from an alcohol to ether, the limitation of ability to interact with IL through hydrogen bonding is observed. In ether, the interaction is most likely due to n- π interaction between the oxygen atom of ether and of imidazolium ring. The possible interaction may be also between the hydrogen at the C₂ position of the imidazole ring, which is known to be the most acidic hydrogen on the ring, and the oxygen atom of the ether. The liquid-liquid equilibria for binary mixtures of [bmim][CH₃SO₄] in three ethers: dipropyl ether, dibutyl ether, and MTBE is shown in Fig. 3. Replacing the alcohol by the ether significantly decreases the solubility at any particular temperature. For [bmim][CH₃SO₄], changes are from complete miscibility in alcohols to close full immiscibility in dibutyl ether. Between these three ethers, the lower UCST of the system was observed for MTBE. This clearly indicates the influence of inductive effects of methyl substituents on the oxygen atom and possible bigger interaction with IL. The influence of different anion on the solubility of [bmim][X], where X = [Cl]⁻, [PF₆]⁻, or [CH₃SO₄]⁻ in dipropyl ether has shown that the two liquid-liquid phase areas decrease in the order: [bmim][PF₆] > [bmim][CH₃SO₄] > [bmim][Cl] [51].

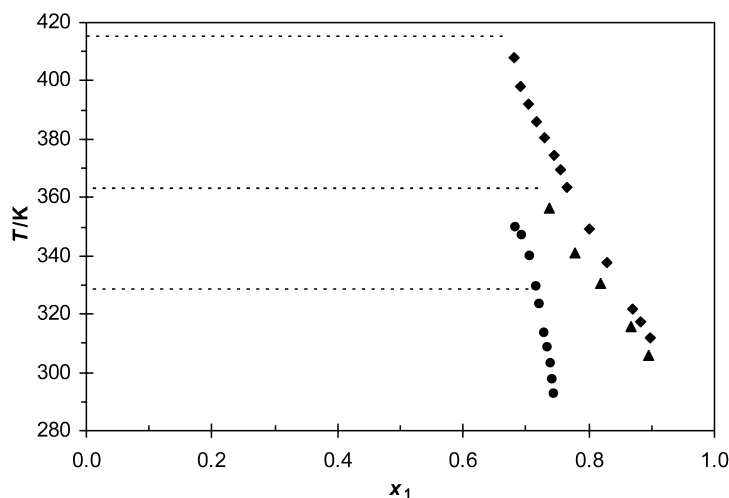


Fig. 3 T-x diagram for [bmim][CH₃SO₄] (1) with ●, MTBE, or ▲, dipropyl ether [51], or ◆, dibutyl ether; dotted line, boiling temperature of a solvent.

Experimental phase diagrams of SLE and LLE for (IL + aromatic hydrocarbon) mixtures discussed in this work are characterized mainly by the following: (1) in all cases, huge miscibility gaps were observed; (2) the mutual solubility of [emim][PF₆] in benzene increases with an increase of the alkyl chain on the imidazole ring ([emim]⁺ vs. [bmim]⁺) (see Fig. 4); the same trend is observed for IL with polar cation [C₆H₁₃OCH₂mim][BF₄] in benzene—the area of immiscibility shifts toward the solvent-rich region; (3) the effect of the anion for [C₆H₁₃OCH₂mim]⁺ ([Tf₂N] vs. [BF₄]) or cation ([bmim]⁺ vs. [emim]⁺) is dramatic (see Fig. 4). Greater mutual solubilities were observed for [C₆H₁₃OCH₂mim][Tf₂N] than for [C₆H₁₃OCH₂mim][BF₄] (see Fig. 4); (4) the influence of the cation's alkyl chain length for two ILs in ethylbenzene is presented in Fig. 5; the trend is similar to the effect observed in alcohols; by lengthening the alkyl chain on the cation from ethyl to butyl

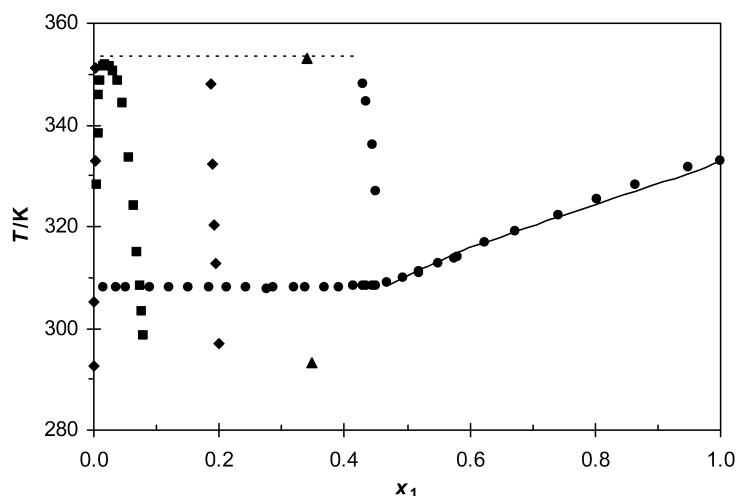


Fig. 4 Solid–liquid and liquid–liquid equilibrium diagrams for different ILs (1) in benzene: ■, $[\text{C}_6\text{H}_{13}\text{OCH}_2\text{mim}][\text{Tf}_2\text{N}]$, or ◆, $[\text{C}_6\text{H}_{13}\text{OCH}_2\text{mim}][\text{BF}_4]$; or ▲, $[\text{bmim}][\text{PF}_6]$ [39]; or ●, $[\text{emim}][\text{PF}_6]$ [39], solid line, calculated by the NRTL equation; dotted line, boiling temperature of benzene.

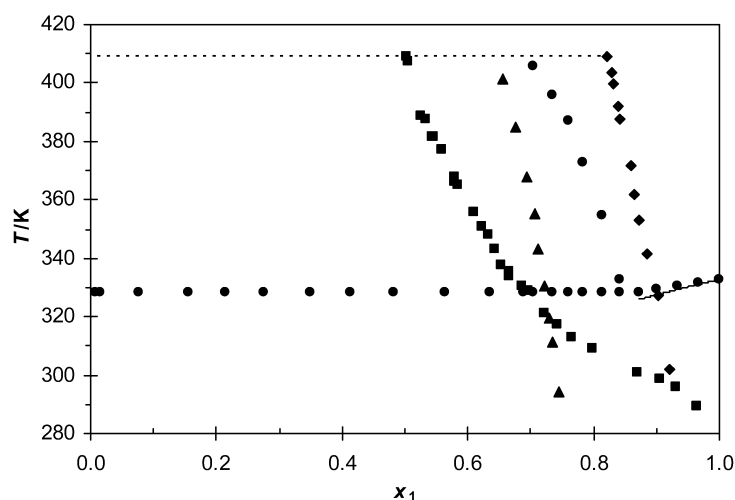


Fig. 5 Solid–liquid and liquid–liquid equilibrium diagrams for different ILs (1) in ethylbenzene: ■, $[\text{bmim}][\text{CH}_3\text{SO}_4]$, or ▲, $[\text{bmim}][\text{PF}_6]$ [39]; or ●, $[\text{emim}][\text{PF}_6]$ [39]; or ◆, $[\text{mmim}][\text{CH}_3\text{SO}_4]$; solid line, calculated by the NRTL equation; dotted line, boiling temperature of ethylbenzene.

($[\text{emim}][\text{PF}_6]$ vs. $[\text{bmim}][\text{PF}_6]$) or from methyl to butyl ($[\text{mmim}][\text{CH}_3\text{SO}_4]$ vs. $[\text{bmim}][\text{CH}_3\text{SO}_4]$) the mutual solubility increases; (5) this trend was also observed for the same ILs in *m*-xylene (see Figs. 6 and 7); the effect of the alkoxy group of cation on the solubility of IL in *m*-xylene is the same as in benzene, but the area of immiscibility is two times bigger in *m*-xylene than in benzene for two different anions (see Figs. 4 and 7); (6) in cyclohexane, this trend is the same (greater mutual solubilities with $[\text{C}_6\text{H}_{13}\text{OCH}_2\text{mim}]^+$ cation than $[\text{emim}]^+$ or $[\text{bmim}]^+$ and $[\text{Tf}_2\text{N}]^-$ anion than the $[\text{BF}_4]^-$ anion (see Fig. 8); the solubility in cyclohexane is much lower than that in aromatic hydrocarbons (benzene, *m*-xylene) which means that the interaction of IL with solvent is lower; (7) the solubility in *n*-heptane is similar to that in cyclohexane; the mutual solubility is bigger for $[\text{bmim}][\text{CH}_3\text{SO}_4]$ than for $[\text{bmim}][\text{PF}_6]$; $[\text{C}_6\text{H}_{13}\text{OCH}_2\text{mim}][\text{BF}_4]$ is more soluble than $[\text{bmim}][\text{CH}_3\text{SO}_4]$ (see Fig. 9); (8) the best solubility is

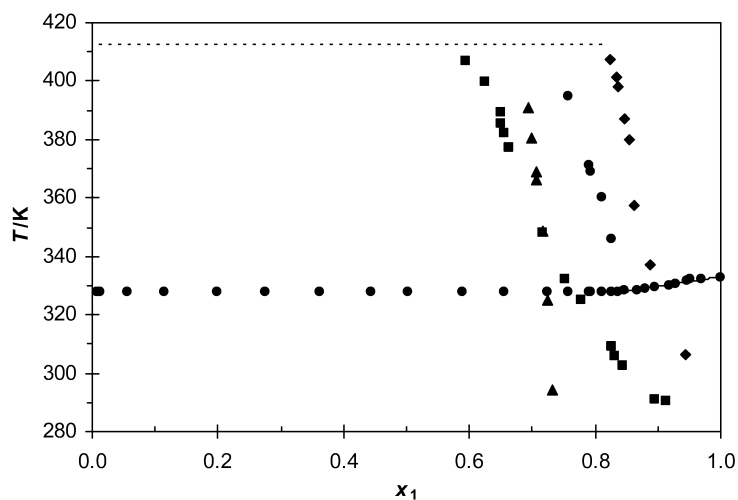


Fig. 6 Solid–liquid and liquid–liquid equilibrium diagrams for different ILs (1) in *m*-xylene: ■, [bmim][CH₃SO₄], or ▲, [bmim][PF₆] [39]; or ●, [emim][PF₆] [39]; or ◆, [mmim][CH₃SO₄]; solid line, calculated by the NRTL equation; dotted line, boiling temperature of *m*-xylene.

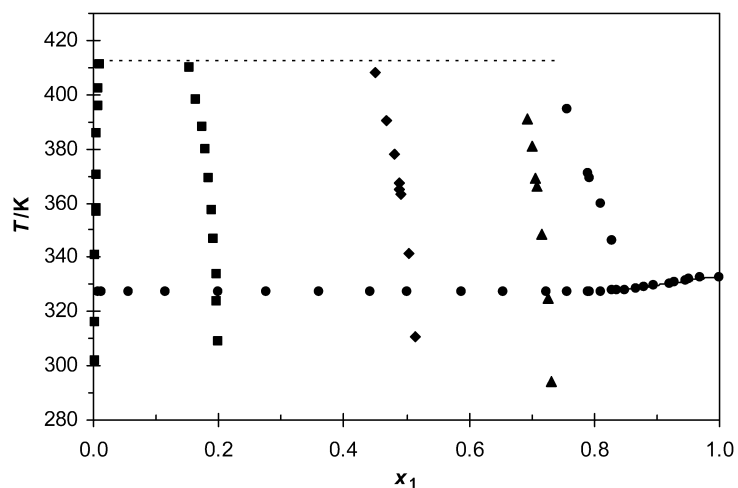


Fig. 7 Solid–liquid and liquid–liquid equilibrium diagrams for different ILs (1) in *m*-xylene: ■, [C₆H₁₃OCH₂mim][Tf₂N], or ◆, [C₆H₁₃OCH₂mim][BF₄]; or ▲, [bmim][PF₆] [39]; or ●, [emim][PF₆] [39], solid line, calculated by the NRTL equation; dotted line, boiling temperature of *m*-xylene.

shown by the [C₆H₁₃OCH₂mim][Tf₂N] in every solvent. The immiscibility gap for alcohols is usually lower than that in benzene; the solubilities in ethers are comparable with solubilities in cyclohexane and in heptane.

Previously, the octan-1-ol/water partition coefficients as a function of temperature and alkyl substituent have been obtained from the solubilities of [almim][Cl], where al = C₄, C₈, C₁₀, and C₁₂ in octan-1-ol and water [48]. The solubility of [almim][Cl], where al = C₁₀, C₁₂ in octan-1-ol is comparable to that of [C₄mim][Cl] in octan-1-ol. Liquid at room temperature [C₈mim][Cl] is not miscible with octan-1-ol and water, thus, the LLE was measured in this system. The differences of solubilities in water for al = C₄ and C₁₂ are not very significant [48]. Additionally, the immiscibility region was observed for the higher concentration of [C₁₀mim][Cl] in water. The intermolecular solute–solvent interaction of [C₄mim][Cl] with water is higher than for other 1-alkyl-3-methylimidazolium chlorides. The values of

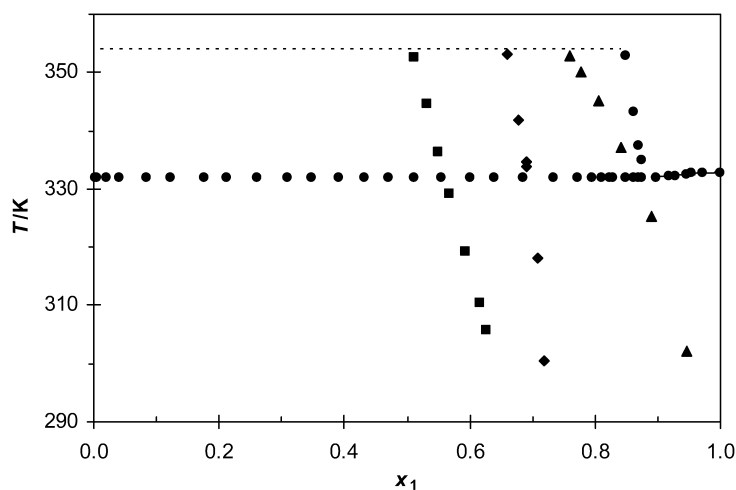


Fig. 8 Solid–liquid and liquid–liquid equilibrium diagrams for different ILs (1) in cyclohexane: ■, $[\text{C}_6\text{H}_{13}\text{OCH}_2\text{mim}][\text{Tf}_2\text{N}]$, or ◆, $[\text{C}_6\text{H}_{13}\text{OCH}_2\text{mim}][\text{BF}_4]$; or ▲, $[\text{bmim}][\text{PF}_6]$ [39]; or ●, $[\text{emim}][\text{PF}_6]$, solid line, calculated by the NRTL equation; dotted line, boiling temperature of cyclohexane.

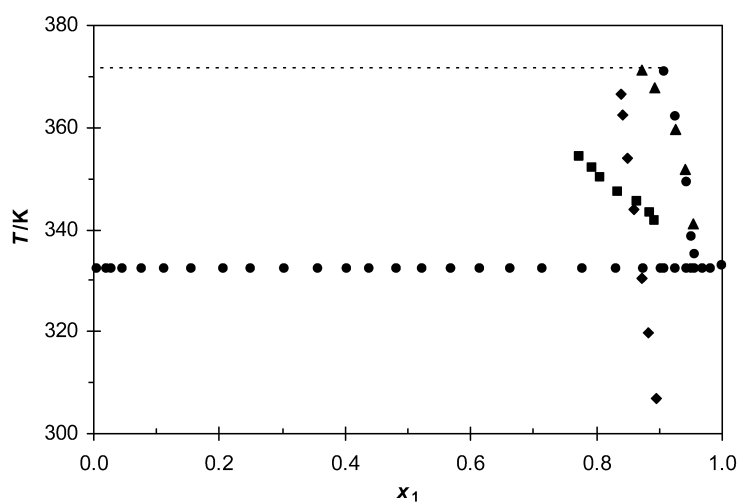


Fig. 9 Solid–liquid and liquid–liquid equilibrium diagrams for different ILs (1) in *n*-heptane: ■, $[\text{bmim}][\text{CH}_3\text{SO}_4]$, or ◆, $[\text{C}_6\text{H}_{13}\text{OCH}_2\text{mim}][\text{BF}_4]$, or ▲, $[\text{bmim}][\text{PF}_6]$ [39]; or ●, $[\text{emim}][\text{PF}_6]$; dotted line, boiling temperature of *n*-heptane.

partition coefficient (P) for 1,3-dialkylimidazolium chloride salts were from 0.48 to 0.73 (at 298.15 K) while for alkyl-(2-hydroxyethyl)-dimethyl-ammonium bromide salts were from 0.16 to 0.64 (at 298.15 K) [61]. Experimental partition coefficients ($\log P$) are negative in three temperatures, which is the evidence of the possibility of using these ILs as green solvents.

Correlation of experimental data

For the LLE, the data obtained for the solvent-rich phases does not authorize to do any calculations in the area of LLE. In many mixtures it was impossible to detect the equilibrium curve at the IL small mole fraction area by the visual method. The observation of the liquid–liquid demixing was inhibited by the

permanently foggy solution. The spectroscopic or other techniques are necessary in the mixtures under study.

The SLE in a mixture of a solid 1 in a liquid may be expressed in a very general manner by eq. 1 [62]

$$-\ln x_1 = \frac{\Delta_{\text{fus}}H_1}{R} \left(\frac{1}{T} - \frac{1}{T_{\text{fus},1}} \right) - \frac{\Delta_{\text{fus}}Cp_{,1}}{R} \left(\ln \frac{T}{T_{\text{fus},1}} + \frac{T_{\text{fus},1}}{T} - 1 \right) + \ln \gamma_1 \quad (1)$$

where x_1 , γ_1 , $\Delta_{\text{fus}}H_1$, $\Delta_{\text{fus}}Cp_{,1}$, $T_{\text{fus},1}$, and T stand for mole fraction, activity coefficient, enthalpy of fusion ($17.86 \text{ kJ}\cdot\text{mol}^{-1}$ for [emim][PF₆] [39]; $14.057 \text{ kJ}\cdot\text{mol}^{-1}$ for [bmim][Cl] [50]), difference in solute heat capacity between the solid and liquid at the melting temperature (this value is unknown), melting temperature of the solute (1) (for [emim][PF₆] $T_{\text{fus},1} = 332.80 \text{ K}$ [39]; for [bmim][Cl] $T_{\text{fus},1} = 341.94 \text{ K}$ [50]), and measured equilibrium temperature, respectively. The melting point of [emim][PF₆] was reported to be $331\text{--}333 \text{ K}$ [63] or 335.15 K [22]. The procedure of correlation was described in our previous papers [39,40,48–51]. In this study, the NRTL 1 [53] model was used to fit the solute activity coefficients, γ_1 to the so-called correlation equations that describe the Gibbs excess free energy of mixing, (G^E), in mixtures with alcohols. The modified form of the NRTL equation proposed by Renon was presented by Nagata and coworkers [53] by substituting local surface fraction for local mole fraction and further by including Guggenheim's combinatorial entropy for athermal mixtures whose molecules differ in size and shape. The resultant equations involve three adjustable parameters and are extended to multicomponent systems without adding ternary parameters. The root-mean-square deviation of temperature (σ_T defined by eq. 2) was used as a measure of the goodness of the solubility correlation

$$\sigma_T = \left(\frac{\sum_{i=1}^n \left[\frac{(T_i)^{\text{exp}} - (T_i)^{\text{cal}}}{n-2} \right]^2}{n-2} \right)^{\frac{1}{2}} \quad (2)$$

where n is the number of experimental points (including the melting point) and 2 is the number of adjustable parameters. The molar volume, V_m , of pure component at 298.15 K (for the hypothetical sub-cooled substance at 298.15 K are: for [emim][PF₆], $V_m = 242.6 \text{ cm}^3\cdot\text{mol}^{-1}$ [39]; for [bmim][Cl] $V_m = 186.70 \text{ cm}^3\cdot\text{mol}^{-1}$ [50]. Table 2 lists the results of fitting the solubility curves by the NRTL1 or NRTL equations together with the values of the parameter α_{12} , a constant of proportionality similar to the non-randomness constant of the NRTL equations.

For the systems presented in this table, the description of SLE for alcohols given by the NRTL1 equation was much worse than that for hydrocarbons by NRTL. The average deviation for alcohols is $\sigma_T = 2.8 \text{ K}$, [40] whilst for hydrocarbons it is $\sigma_T = 0.41 \text{ K}$ [39]. The correlation of the LLE using the same parameters from the same models is quite difficult in this work because of the lack of the experimental points in the solvent-rich region. Parameters shown in Table 2 may be helpful for describing the activity coefficients for any concentration, temperature, and for the description of ternary mixtures. They are also useful for the complete thermodynamic description of the solution.

Table 2 Correlation of the SLE data of the {[bmim][Cl] or [emim][PF₆](1) + solvent (2)} binary mixtures by the NRTL and NRTL 1 equations: values of parameters and measures of deviations [39,40].

System	Parameters	Deviations
IL + solvent	$\Delta g_{12}/\Delta g_{21}$ J mol ⁻¹	σ_T^a K
[bmim][Cl] + butan-1-ol ^b	-50364/-8656	2.58
[emim][PF ₆] + butan-1-ol ^c	2538/-3040	0.67
[emim][PF ₆] + benzene ^d	2468/184.1	0.76
[emim][PF ₆] + ethylbenzene ^d	-1105/5168	0.09
[emim][PF ₆] + <i>m</i> -xylene ^d	4734/66421	0.57
[emim][PF ₆] + cyclohexane ^d	18982/-7278	0.23

^aAccording to eq. 2 in the text.

^b $\alpha = 0.3$.

^c $\alpha = 0.95$.

^d $\alpha = 0.8$.

CONCLUDING REMARKS

ILs can be considered, in the majority of cases, as polar phases with their solvent properties being mainly determined by the ability of the salt to act as a hydrogen-bond donor and/or acceptor and the degree of localization of the charges on the anions. In most cases, imidazolium-based ILs are highly ordered hydrogen-bonded substances and can have strong effects on chemical reactions and processes. Thus, the ability of IL to form hydrogen bonds or other possible interactions with potential solvents is an important feature of its behavior. Additionally, ILs are such good hydrogen-bond donors/acceptors because they are charged, which was mentioned above. Alcohols used in this work are also good hydrogen-bond donors/acceptors, but not as good as ILs. Greater interaction was observed for [C₆H₁₃OCH₂mim][Tf₂N] with benzene, *m*-xylene, and cyclohexane than for [C₆H₁₃OCH₂mim][BF₄] with these solvents. We believe this was due to stronger interaction of the [Tf₂N] anion than the [BF₄] anion with the solvent. Therefore, the choice of anion can have a huge effect on the phase behavior of imidazolium ILs not only with alcohols [58], but also with hydrocarbons. The specific interaction with solvent (between the nitrogens of the imidazole ring and oxygen of the alkoxymethyl group of cation [C₆H₁₃OCH₂mim] and benzene ring) diminish the area of immiscibility below 0.2 IL mole fraction (in benzene and *m*-xylene), which was shown in Fig. 4.

In polar solvents like alcohols, one can expect stronger interaction with the solvent and possible ruin of the hydrogen-bonded net equally of the solute and the solvent. Clearly, hydrogen bonding or $n-\pi$, or other interaction of cation or anion of IL with solvent, plays an important role in controlling liquid–liquid and solid–liquid phase behavior of imidazolium-based ILs. However, the existence of the liquid–liquid phase equilibria in these mixtures is the evidence that the interaction between the IL and the solvent is not significant.

The ([emim][PF₆] + methanol) binary mixture exhibited simple eutectic system [40]. The liquid–liquid phase diagrams for the mixtures under study exhibited USCT. In many mixtures, the observations of USCT were limited by the boiling temperature of the solvent. Sometimes it was impossible to detect by the visual method the mutual solubility of ILs with the solvent in the solvent-rich phase. Such an observation in the solvent-rich region was not possible, for example, for the [emim][PF₆] in butan-2-ol, *tert*-butanol, and 3-methylbutan-1-ol alcohols [40] and for most of the mixtures with [m or bmim][CH₃SO₄] salts. The spectroscopic or other techniques are necessary in the mentioned mixtures.

As compared to conventional organic solvents, ILs are much more complex solvents capable of undergoing many types of interactions. Characterizing them with a single "polarity" term fails to describe the type and magnitude of individual interactions that make each IL unique.

ACKNOWLEDGMENTS

This research has been supported by the Polish Committee for Scientific Research (Grant 3 T09B 004 27). The author would like to thank A. Marciniak and A. Pobudkowska for cooperation and Prof. J. Pernak for the synthesis of the $[C_6H_{13}OCH_2mim][BF_4]$ and $[C_6H_{13}OCH_2mim][Tf_2N]$ samples.

REFERENCES

1. J. Dupont, R. F. De Souza, P. A. Suarez. *Chem. Rev.* **102**, 3667 (2002).
2. Ch. J. Adams, M. J. Earle, K. R. Seddon. *Green Chem.* **2**, 21 (2000).
3. J. L. Scott, D. R. MacFarlane, C. L. Raston, Ch. M. Teoh. *Green Chem.* **2**, 123 (2000).
4. J. D. Holbrey, K. R. Seddon, R. Wareing. *Green Chem.* **3**, 33 (2000).
5. R. Sheldon. *Chem. Commun.* 2399 (2002).
6. P. A. Z. Suarez, J. R. L. Dullius, S. Einloft, R. F. De Souza, J. Dupont. *Polyhedron* **7**, 1217 (1996).
7. Y. Chauvin and H. Olivier-Bourbigou. *CHEMTECH* **26** (1995).
8. J. Dupont, P. A. Z. Suarez, R. F. De Souza, R. A. Burrow, J.-P. Kintzinger. *Chem. Eur. J.* **6**, 2377 (2000).
9. P. Wasserscheid and W. Keim. *Angew. Chem., Int. Ed.* **39**, 3773 (2000).
10. R. S. Varma and V. V. Namboodiri. *Chem. Commun.* 643 (2001).
11. F. Zulfigar and T. Kitazume. *Green Chem.* **2**, 137 (2000).
12. F. Zulfigar and T. Kitazume. *Green Chem.* **2**, 296 (2000).
13. C. W. Lee. *Tetrahedron Lett.* **40**, 2461 (1999).
14. J. Holbrey and K. R. Seddon. *Clean Prod. Process.* **1**, 223 (1999).
15. L. C. Branco, J. N. Rosa, J. J. M. Ramos, C. A. M. Afonso. *Chem. Eur. J.* **8**, 3671 (2002).
16. J. H. Werner, S. N. Baker, G. A. Baker. *Analyst* **128**, 786 (2003).
17. S. N. Baker, G. A. Baker, F. V. Bright. *Green Chem.* **4**, 165 (2002).
18. A. E. Bradley, C. Hardacre, J. D. Holbrey, S. Johnston, S. E. J. McMath, M. Nieuwenhuyzen. *Chem. Mater.* **14**, 629 (2002).
19. S. V. Dzyuba and R. A. Bartsch. *Chem. Phys. Chem.* **3**, 161 (2002).
20. J. L. Anthony, E. J. Maginn, J. F. Brennecke. *J. Phys. Chem. B* **105**, 10942 (2001).
21. B. Wu, R. G. Reddy, R. D. Rogers. *Solar Forum 2001, Solar Energy: The Power to Choose*, 21–25 April 2001, Washington, DC (2001).
22. H. L. Ngo, K. LeCompte, L. Hargens, A. B. McEwen. *Thermochim. Acta* **357–358**, 97 (2000).
23. S. N. Baker, G. A. Baker, M. A. Kane, F. V. Bright. *J. Phys. Chem. B* **105**, 9663 (2001).
24. G. Law and P. R. Watson. *Chem. Phys. Lett.* **1**, 345 (2001).
25. J. Dupont, C. S. Consorti, J. Spencer. *J. Braz. Chem. Soc.* **11**, 337 (2000).
26. S. N. V. K. Aki, J. F. Brennecke, A. Samanta. *Chem. Commun.* 413 (2001).
27. M. Koel. *Proc. Estonian Acad. Sci. Chem.* **3**, 145 (2000).
28. P. A. Z. Suarez, S. Einloft, J. E. L. Dullius, R. F. De Souza, J. Dupont. *J. Chim. Phys.* **95**, 1626 (1998).
29. J. Fuller, R. T. Carlin, R. A. Osteryoung. *J. Electrochem. Soc.* **144**, 3881 (1997).
30. M. Kosmulski, R. A. Osteryoung, M. Ciszowska. *J. Electrochem. Soc.* **147**, 1454 (2000).
31. N. Papagerogiou, Y. Athanassov, M. Armand, P. Bonhôte, H. Pettersson, A. Azam, M. Grätzel. *J. Electrochem. Soc.* **143**, 3099 (1996).
32. U. Schröder, J. D. Wadhawan, R. G. Compton, F. Marken, P. A. Z. Suarez, C. S. Consorti, R. F. De Souza, J. Dupont. *New J. Chem.* **24**, 1009 (2000).

33. A. P. Abbott and D. J. Schiffrin. *J. Chem. Soc., Faraday Trans.* **86**, 1453 (1990).
34. D. R. McFarlane, J. Sun, J. Golding, P. Meakin, M. Forsyth. *Electrochem. Acta* **45**, 1271 (2000).
35. J. G. Huddleston, H. D. Willauer, R. P. Swatloski, A. E. Visser, R. D. Rogers. *Chem. Commun.* 1765 (1998).
36. S. Dai, Y. H. Ju, C. E. Barnes. *J. Chem. Soc., Dalton Trans.* 1201 (1999).
37. A. E. Visser, R. P. Swatloski, R. D. Rogers. *Green Chem.* **2**, 1 (2000).
38. T. M. Letcher and N. Deenadayalu. *J. Chem. Thermodyn.* **35**, 67 (2003).
39. U. Domańska and A. Marciniak. *J. Chem. Eng. Data* **48**, 451 (2003).
40. U. Domańska and A. Marciniak. *J. Phys. Chem. B* **108**, 2376 (2004).
41. K. N. Marsh, A. Deev, C.-T. Wu, E. Tran, A. Klamt. *Kor. J. Chem. Eng.* **19**, 357 (2002).
42. V. Najdanovic-Visak, J. M. S. Esperanca, L. P. N. Rebelo, M. N. da Ponte, H. J. R. Guedes, K. R. Seddon, R. F. de Souza, J. Szydłowski. *J. Phys. Chem B* **107**, 12797 (2003).
43. J. M. Crosthwaite, S. N. V. Aki, E. J. Maginn, J. F. Brennecke. *Fluid Phase Equilib.* (2005). In press.
44. W. Arlt, M. Seiler, G. Sadowski, H. Frey, H. Kautz. DE patent no. 10160518.8.
45. M. Krummen and J. Gmehling. 17th IUPAC Conference on Chemical Thermodynamics, 28.07-02.08, 2002, Rostock, Germany.
46. G.-T. Wei, Z. Yang, Ch-J. Chen. *Anal. Chim. Acta* **488**, 183 (2003).
47. U. Domańska, E. Bogel-Łukasik, R. Bogel-Łukasik. *J. Phys. Chem. B* **107**, 1858 (2003).
48. U. Domańska, E. Bogel-Łukasik, R. Bogel-Łukasik. *Chem. Eur. J.* **9**, 3033 (2003).
49. U. Domańska and E. Bogel-Łukasik. *Ind. Eng. Chem. Res.* **42**, 6986 (2003).
50. U. Domańska and E. Bogel-Łukasik. *Fluid Phase Equilib.* **218**, 123 (2004).
51. U. Domańska and L. Mazurowska. *Fluid Phase Equilib.* **221**, 73 (2004).
52. G. M. Wilson. *J. Am. Chem. Soc.* **86**, 127 (1964).
53. J. Nagata, Y. Nakamiya, K. Katoh, J. Koyabu. *Thermochim. Acta* **45**, 153 (1981).
54. D. S. Abrams and J. M. Prausnitz. *AIChE J.* **21**, 116 (1975).
55. J. Pernak, A. Cepukowicz, R. Poźniak. *Ind. Eng. Chem. Res.* **40**, 2379 (2001).
56. J. Pernak, J. Zabielska-Matejuk, A. Kropacz, J. Foksowicz-Flaczyk. *Holzforshung* **58**, 286 (2004).
57. A. Heintz, J. K. Lehmann, C. Wertz. *J. Chem. Eng. Data* **48**, 472 (2003).
58. J. M. Crosthwaite, S. N. V. Akai, E. J. Maginn, J. F. Brennecke. *J. Phys. Chem. B* **108** (16), 5113 (2004).
59. C.-T. Wu, K. N. Marsh, A. V. Deev, J. A. Boxall. *J. Chem. Eng. Data* **48**, 486 (2003).
60. M. Wagner, O. Stanga, W. Schroer. *Phys. Chem. Chem. Phys.* **5**, 3943 (2003).
61. U. Domańska and R. Bogel-Łukasik. *J. Chem. Phys. B* (2004). Submitted for publication.
62. R. F. Weimar and J. M. Prausnitz. *J. Chem. Phys.* **42**, 3643 (1965).
63. H. Renon and J. M. Prausnitz. *AIChE J.* **14**, 135 (1968).